

Supporting information for:

Limits for resolving isobaric tandem mass tag reporter ions using phase constrained spectrum deconvolution

Christian D. Kelstrup¹, Konstantin Aizikov², Tanveer S. Battth¹,
Arne Kreutzman², Dmitry Grinfeld², Oliver Lange², Daniel Mourad²,
Alexander A. Makarov², and Jesper V. Olsen^{*1}

- 1) The Novo Nordisk Foundation Center for Protein Research,
University of Copenhagen, DENMARK
- 2) Thermo Fisher Scientific, Bremen, GERMANY

* Corresponding author: jesper.olsen@cpr.ku.dk

Table of contents:

- Figure S-1: Characteristics of transient lengths and FT processing method
- Figure S-2: Additional data on precision and accuracy
- Figure S-3: Additional data on intensity dependency
- Table S-1: Overview of acquired raw data

Figure S-1

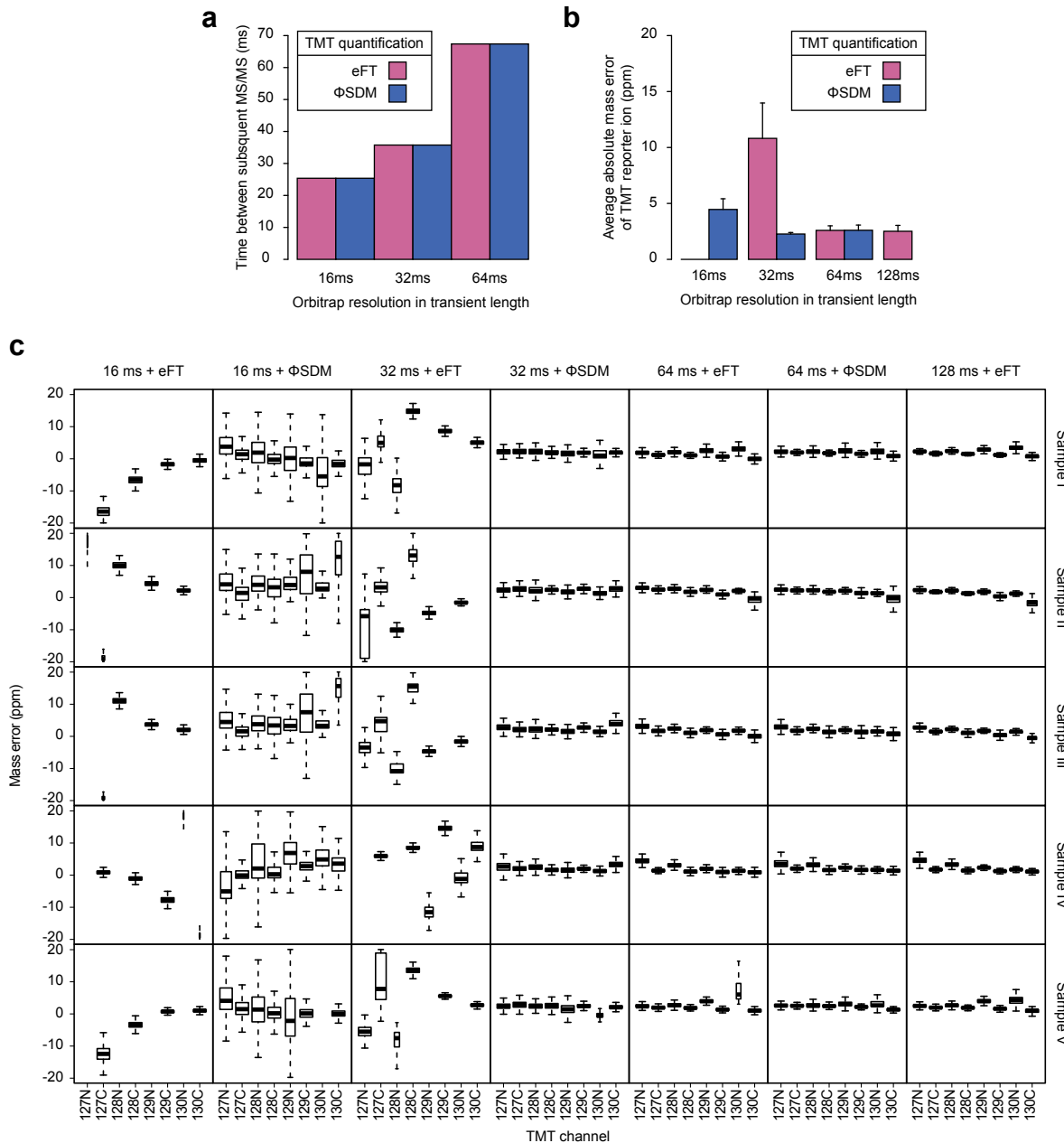


Figure S-1: Characteristics of transient lengths and FT processing method. (a) Bar chart showing the acquisition time for three transients processed with eFT or Φ SDM. There is no difference seen between the eFT and Φ SDM. (b) Bar chart showing a representative example of the average absolute mass accuracy for the 128N reporter ion across different transients. The error bars are the standard deviation from the different samples. The mass accuracy is similar for the 32 ms Φ SDM method and for all longer transients disregarding TMT quantification method. The 16 ms eFT method did not resolve the 128N reporter ion. (c) Boxplots showing details of mass errors for each TMT channel in each sample. The relative widths of the boxes making up each subplot was set proportional to the number of observations in the groups with a lower limit of 1% i.e. narrow boxes indicate a low number of mass error measurements and missing boxes indicate below 1% of peaks were resolved.

Figure S-2

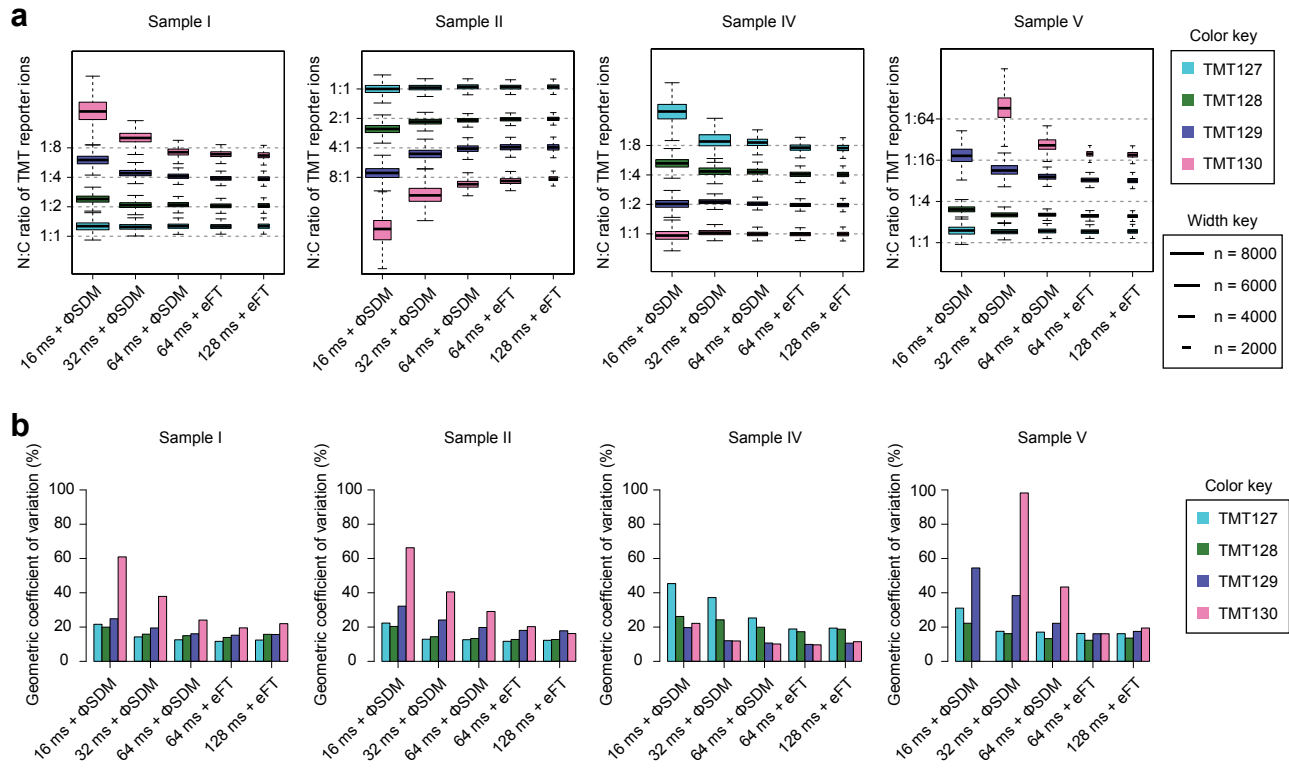


Figure S-2: Additional data on precision and accuracy. (a) Box chart show the quantitative performance for the four N:C ratios across the remaining samples (I, II, IV, and V) and across the five acquisition methods. The width of each box is set proportional to the number of quantified ratios (see width key). (b) Bar chart show the precision in the form of the geometric coefficient of variation for the observed ratios for each reporter ion pair.

Figure S-3

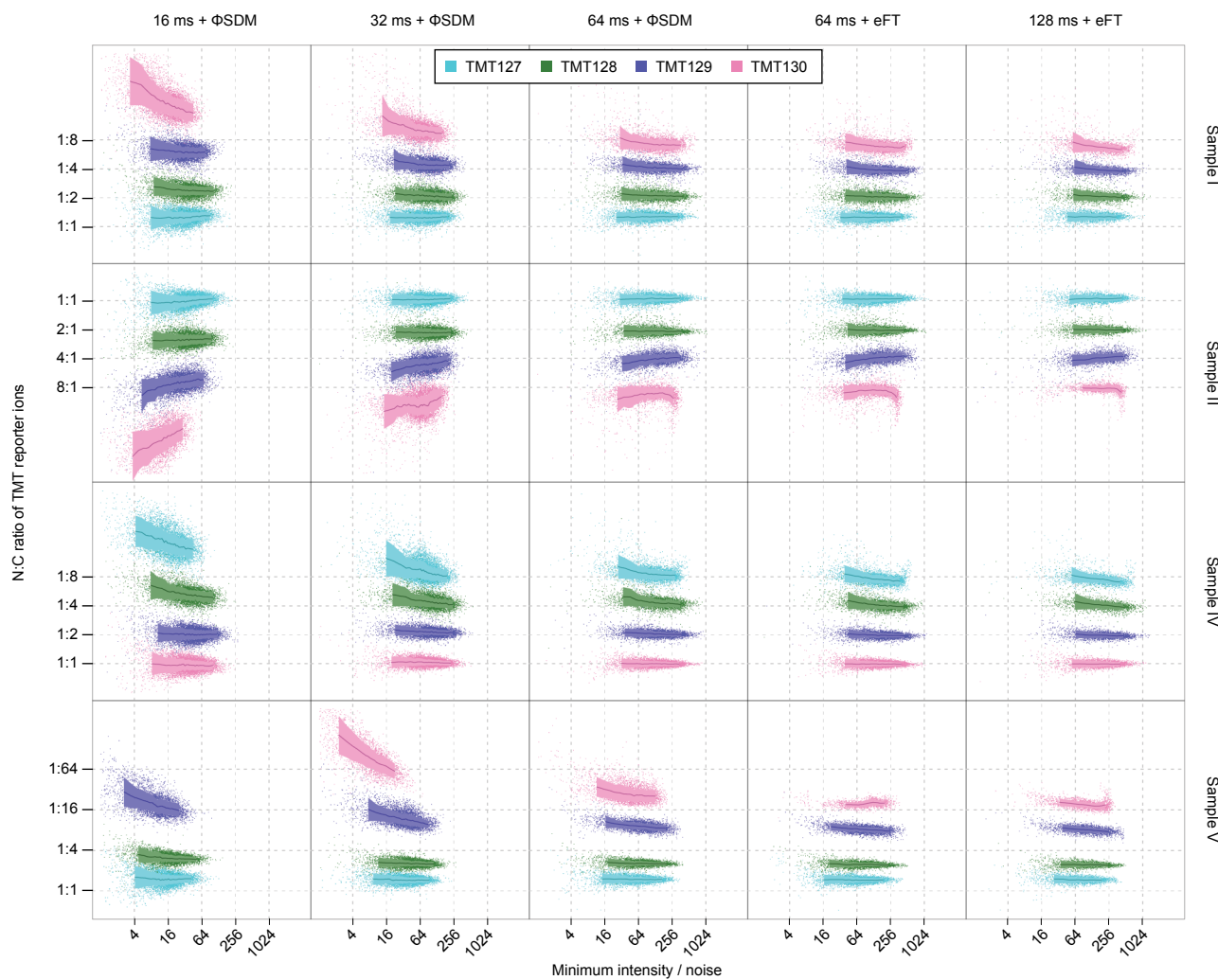


Figure S-3: Additional data on intensity dependency. Scatter plot showing the observed N:C ratios for each closely spaced TMT reporter ion pair as a function of the minimum intensity to noise value. An overlay has been added to show trends, consisting of a darkened line representing the 300 point moving average and a solid area covering the moving average \pm the moving standard deviation. The four samples not detailed in the main text are shown here for each of the five acquisition methods.

Table S-1 (1/7): Overview of acquired raw data

Table S-1 (2/7): Overview of acquired raw data

Table S-1 (3/7): Overview of acquired raw data

Table S-1 (4/7): Overview of acquired raw data

Table S-1 (5/7): Overview of acquired raw data

Table S-1 (6/7): Overview of acquired raw data

Table S-1 (7/7): Overview of acquired raw data

Raw file	Experiment	Sample	MS method	Gradient
20180823_QE3_nLC3_ChKe_SA_TMT_Frac42_eFT_1	Fractionation	4 cell lines, fraction 42	eFT, 64 ms transient, 54 ms ion injection	15min
20180823_QE3_nLC3_ChKe_SA_TMT_Frac42_eFT_2	Fractionation	4 cell lines, fraction 42	eFT, 64 ms transient, 54 ms ion injection	15min
20180823_QE3_nLC3_ChKe_SA_TMT_Frac42_phi_1	Fractionation	4 cell lines, fraction 42	ΦSDM, 32 ms transient, 22 ms ion injection	15min
20180823_QE3_nLC3_ChKe_SA_TMT_Frac42_phi_2	Fractionation	4 cell lines, fraction 42	ΦSDM, 32 ms transient, 22 ms ion injection	15min
20180823_QE3_nLC3_ChKe_SA_TMT_Frac43_eFT_1	Fractionation	4 cell lines, fraction 43	eFT, 64 ms transient, 54 ms ion injection	15min
20180823_QE3_nLC3_ChKe_SA_TMT_Frac43_eFT_2	Fractionation	4 cell lines, fraction 43	eFT, 64 ms transient, 54 ms ion injection	15min
20180823_QE3_nLC3_ChKe_SA_TMT_Frac43_phi_1	Fractionation	4 cell lines, fraction 43	ΦSDM, 32 ms transient, 22 ms ion injection	15min
20180823_QE3_nLC3_ChKe_SA_TMT_Frac43_phi_2	Fractionation	4 cell lines, fraction 43	ΦSDM, 32 ms transient, 22 ms ion injection	15min
20180823_QE3_nLC3_ChKe_SA_TMT_Frac44_eFT_1	Fractionation	4 cell lines, fraction 44	eFT, 64 ms transient, 54 ms ion injection	15min
20180823_QE3_nLC3_ChKe_SA_TMT_Frac44_eFT_2	Fractionation	4 cell lines, fraction 44	eFT, 64 ms transient, 54 ms ion injection	15min
20180823_QE3_nLC3_ChKe_SA_TMT_Frac44_phi_1	Fractionation	4 cell lines, fraction 44	ΦSDM, 32 ms transient, 22 ms ion injection	15min
20180823_QE3_nLC3_ChKe_SA_TMT_Frac44_phi_2	Fractionation	4 cell lines, fraction 44	ΦSDM, 32 ms transient, 22 ms ion injection	15min
20180823_QE3_nLC3_ChKe_SA_TMT_Frac45_eFT_1	Fractionation	4 cell lines, fraction 45	eFT, 64 ms transient, 54 ms ion injection	15min
20180823_QE3_nLC3_ChKe_SA_TMT_Frac45_eFT_2	Fractionation	4 cell lines, fraction 45	eFT, 64 ms transient, 54 ms ion injection	15min
20180823_QE3_nLC3_ChKe_SA_TMT_Frac45_phi_1	Fractionation	4 cell lines, fraction 45	ΦSDM, 32 ms transient, 22 ms ion injection	15min
20180823_QE3_nLC3_ChKe_SA_TMT_Frac45_phi_2	Fractionation	4 cell lines, fraction 45	ΦSDM, 32 ms transient, 22 ms ion injection	15min
20180823_QE3_nLC3_ChKe_SA_TMT_Frac46_eFT_1	Fractionation	4 cell lines, fraction 46	eFT, 64 ms transient, 54 ms ion injection	15min
20180823_QE3_nLC3_ChKe_SA_TMT_Frac46_eFT_2	Fractionation	4 cell lines, fraction 46	eFT, 64 ms transient, 54 ms ion injection	15min
20180823_QE3_nLC3_ChKe_SA_TMT_Frac46_phi_1	Fractionation	4 cell lines, fraction 46	ΦSDM, 32 ms transient, 22 ms ion injection	15min
20180823_QE3_nLC3_ChKe_SA_TMT_Frac46_phi_2	Fractionation	4 cell lines, fraction 46	ΦSDM, 32 ms transient, 22 ms ion injection	15min